www.sciencemag.org/cgi/content/full/338/6106/524/DC1

Supplementary Materials for

Maturation-Dependent HIV-1 Surface Protein Redistribution Revealed by Fluorescence Nanoscopy

Jakub Chojnacki, Thorsten Staudt, Bärbel Glass, Pit Bingen, Johann Engelhardt, Maria Anders, Jale Schneider, Barbara Müller, Stefan W. Hell, Hans-Georg Kräusslich*

*To whom correspondence should be addressed. E-mail: hans-georg.kraeusslich@med.uni-heidelberg.de

Published 26 October 2012, *Science* **338**, 524 (2012)
DOI: 10.1126/science.1226359

This PDF file includes:

Materials and Methods

Viruses and cell lines

Replication incompetent HIV-1 particles were produced by transfection of plasmid pCHIV (*27*) expressing all HIV-1_{NL4-3} proteins except Nef and lacking the viral long terminal repeat regions. Derivatives of this plasmid with a frameshift and premature termination of Env (pCHIV Env(-)) as well as variants containing either a mutation in the PR active site (pCHIV PR(-)) or at specific PR cleavage sites in Gag (pCHIV (MA-CA) and pCHIV (CA-p6)) have been described previously (*27, 28*). Pseudotyping was performed using plasmid pCAGGS expressing either wild type Env (Env(wt)) or an Env variant with a 144 amino acid truncation of its C-terminal tail (Env(ΔCT)) (*22*). Infectious HIV particles were generated using pNL4-3 (*29*) or pNL4-3CTdel-144-2 (a kind gift from C. Aiken (*3*)) carrying wt Env or Env(ΔCT), respectively. Reporter particles for virus entry assays were generated by cotransfection of pCHIV or pCHIV (MA-p6), an expression vector for either wt Env or Env(ΔCT), and plasmid pMM310, encoding a β-lactamase-Vpr fusion protein (provided by N. Landau). Plasmid eGFP.Vpr (*16*) was provided by Tom Hope.

293T cells were grown in Dulbecco's modified Eagle's medium (DMEM) (Invitrogen), supplemented with 10% fetal calf serum, 100 U/ml penicillin-streptomycin and 20 mM HEPES pH 7.4. MT-4 (*30*), C8166 and SupT1-CCR5 (SupT1R5) (*31*) cells were maintained in RPMI medium supplemented as above with the addition of 0.3 μg/ml puromycin. Cells were maintained at 37°C, 5% CO_2.

Antibodies and Fab fragments

Sheep polyclonal anti-CA antiserum was raised against recombinant HIV-1 CA. Human anti-gp120 monoclonal antibodies 2G12 and b12 were purchased from Polymun Scientific; polyclonal rabbit anti-gp120 and anti-CD4 antibodies were a kind gift from Valerie Bosch, Heidelberg. The humanized anti-respiratory syncytial virus F protein antibody (Synagis) was obtained from Abbott. Fab fragments were generated from respective IgGs using the Fab Micro Preparation

kit (Pierce) according to the manufacturer's instructions. The quality of Fab preparations was analyzed by SDS-PAGE and Coomassie staining. Anti-human and anti-rabbit IgG Fab fragments (Jackson ImmunoResearch) were coupled to Atto 565 (Atto-Tec) and Dy-485XL (Dyomics GmbH) dyes via NHS-ester chemistry according to the dye manufacturer's instructions.

Particle preparation

Virus particles were prepared from the tissue culture supernatant of 293T cells co-transfected using polyethyleneimine (PEI) with 14 µg pNL4-3 or pCHIV (or the respective mutated derivative) and 1 µg peGFP.Vpr or 2.5 µg pMM310 per 10 cm dish, respectively. For pseudotyped particles, 15 µg of pCHIV Env(-), 1µg of peGFP.Vpr and 2.5 µg of the indicated Env expression plasmid were used. Infectious HIV-1 particles for biochemical determination of Env incorporation were produced from infected MT-4 T-cells; immature particles were produced in the presence of 2 µM of the HIV protease inhibitor lopinavir.

Tissue culture supernatants were harvested 48 h after transfection or infection, cleared by filtration through a 0.45 µm nitrocellulose filter, and particles were purified by centrifugation through a 20% (w/w) sucrose cushion at 70,000 g for 2 h at 4 °C. Particles used for bulk Env incorporation quantitation were further purified by ultracentrifugation through a 6-35% Optiprep (Axis-Shield) gradient at 175,000 g for 90 min at 4 °C (*32*). Purity of gradient purified virus preparations was confirmed by SDS-PAGE followed by silver staining.Virus containing gradient fractions were diluted in phosphate buffered saline (PBS) and pelleted at 260,000 g for 45 min at 4 °C. Particles were resuspended in ice-cold 20 mM HEPES/PBS pH 7.4, frozen rapidly in liquid nitrogen and stored in aliquots at −80 °C.

STED microscope setup

All STED microscope setups used for this study were custom-built. Pulsed excitation of the Atto 565 (Atto-Tec) label was achieved using a high-repetition rate laser source PicoTA (PicoQuant) at a wavelength of λ_{exc}=532 nm, synchronized with the STED-laser via a photodiode (Alphalas).

Dy-485XL (Dyomics GmbH) and eGFP were excited by the 470 nm line from a pulsed high-repetition rate laser diode source (PicoQuant). Fluorescence inhibition at λ_{STED}=647 nm was accomplished using an actively mode locked (APE) Ar-Kr laser (Spectra Physics-Division of Newport Corporation). Beams were combined using acousto-optical tunable filters (AOTF) (Crystal Technologies) and coupled into a microscope stand (DMI 4000B, Leica Microsystems CMS GmbH) equipped with a three axis piezo stage-scanner (PI) and an ACS APO, 63x/1.30NA oil immersion lens (Leica Microsystems CMS GmbH). AOTFs enable blanking of the lasers and allow the power of each laser beam to be controlled independently. They also provide a means for selecting counter-propagating fluorescence returning from the confocal microscope. The collected fluorescence was passed through an additional band-pass filter (580/40 for Atto 565 / Dy-485XL and 510/40 for eGFP (AHF Analysentechnik)) and was detected confocally with a single-photon counting module (SPCM-AQR-13-FC, PerkinElmer). The scanner fly backs were blanked via the line signal from the Imspector data acquisition software. A vortex phase plate (RPC Photonics) was used in the STED beam path to generate a donut shaped focal intensity distribution.
For the GFP-STED setup, excitation was achieved with a pulsed diode laser at 485 nm (PicoQuant GmbH). The excitation source was triggered by a pulsed STED source (MPB Communications Inc.) operating at the wavelength of 560 nm. The excitation and STED beams were combined on a longpass filter (561 nm; Semrock Inc.). Beams were coupled into the microscope stand (Leica Microsystems CMS GmbH) equipped with the oil objective lens HCX PL Apo 100x (Leica MicrosystemsCMS GmbH). Four galvanometer mirrors (Cambridge Technologies) scanned the beams across the sample in x and y direction. The fluorescence signal was separated from the excitation and STED beams via a bandpass filter (525/50; Chroma Technology Corp.) at the entrance of the microscope and via a second bandpass filter (525/45; Semrock Inc.) at the entrance of the detection path. The fluorescence was detected by a hybrid photodetector (Hamamatsu Photonics). A field-programmable gate array (FPGA) based data processing unit was used to sample the output signal of the detector and to reconstruct the image. A vortex phase plate (RPC Photonics) was used in the STED beam path to generate a donut shaped focal intensity distribution.

Immunofluorescence staining

Purified particles (~1 µg of CA) were adhered to fibronectin (100 µg/µL; Sigma) coated glass cover slips for 30 min. Cover slips were blocked using 2% bovine serum albumin (BSA) (Sigma)/PBS for 30 min. Particles were stained for Env using 10 ng/µL 2G12 Fab fragments or b12 Fab fragments, respectively, and anti-human Atto 565 conjugated Fab fragments. Following immunostaining, particles were washed in PBS, briefly fixed using 3% PFA/PBS, overlaid with 1,4-diazabicyclo[2.2.2]octane (DABCO)/MOWIOL and imaged using STED microscopy. All steps were carried out at room temperature.

For detection of cell-attached particles, SupT1R5 cells were adhered to PEI-coated cover slips for 1 h at 37 °C. All subsequent steps were carried out at 16 °C. Equal amounts of the indicated virus particles (~1 µg of CA) from two independent virus preparations were pre-bound to 1 µg of 2G12 Fab fragments for 1 h then added to cells and incubated for 2 h. Subsequently, cells were washed three times with PBS, followed by blocking using 2% BSA/PBS for 15 min and immunostaining for Env and CD4 using rabbit-anti CD4 Fab fragments and anti-rabbit Dy-485XL conjugated Fab fragments as well as anti-human Atto 565 conjugated Fab fragments. Following immunostaining, particles were washed in PBS, briefly fixed using 3% PFA/PBS, embedded in 1,4-diazabicyclo[2.2.2]octane (DABCO)/MOWIOL and imaged using STED microscopy.

Image acquisition and processing

Images for each channel were acquired sequentially with the diffraction limited eGFP.Vpr signal acquired prior to Atto 565 (HIV-1 Env) or Dy-485XL (CD4) signals, respectively, to minimize eGFP exposure to the STED laser. The eGFP signal was generally acquired in a conventional confocal microscope mode (with STED laser turned off) whereas the Atto 565 and Dy-485XL signals were acquired in STED or conventional confocal microscopy modes. The following parameters were used during image acquisition: pinhole size: 1 Airy; dwell time: 300 µs/pixel; field of view: 5 µm x 5 µm and pixel size: 19.9 nm. All images were processed (background subtracted) using Imspector software (www.imspector.de). STED images were

noise filtered using a Richardson-Lucy algorithm (*33*) using Lorentzian PSF of 40 nm FWHM in XY dimensions. This represents an estimate of the system's effective PSF as confirmed by measurements of single monomeric Env proteins immunolabelled with Atto 565 (Fig. S2).
For the GFP-STED measurement, the eGFP signal was acquired in both confocal mode (with STED laser turned off) and STED mode. The following parameters were used during the image acquisition: slit confocality with a width of 1 Airy; dwell time: 40 µs/pixel with 20 µs each during forward and backwards scanning of the beam; field of view: 10 µm x 10 µm and pixel size: 20 nm. All images were processed (background subtracted) using Imspector software.

Quantitation of Env incorporation

Recombinant Env proteins were a kind gift from P. Guardado-Calves, Paris. For STED reference samples, Atto 565 labelled anti-human Fab fragments as well as ~2.5 ng of recombinant monomeric or trimeric Env (gp140), respectively, were adhered to poly-Lysine (Sigma) coated cover slips for 30 min. Cover slips were blocked using 2% BSA (Sigma)/PBS for 30 min. Recombinant gp140 samples were stained using 10 ng/µL 2G12 Fab fragments and anti-human Atto 565 conjugated Fab fragments. Background subtracted photon count integrals for individual complexes were acquired using a 160 nm x 160 nm area from the raw image data. Virus samples, stained for Env using the standard labeling protocol, were analyzed in parallel. Background subtracted Env fluorescence intensity integrals for individual particles were acquired from the raw Env signal using the noise filtered Env signal as a guide. The number of Env trimers per particle was estimated based on the average fluorescence intensity of the recombinant trimeric gp140 reference sample.
For quantitative immunoblotting, samples were separated by SDS-PAGE (12.5% acrylamide) and transferred onto a nitrocellulose membrane (Whatman) by semi-dry blotting. Virus derived proteins were detected by sheep polyclonal anti-CA serum or rabbit polyclonal anti-gp120 serum, respectively. Detection of viral protein bands was performed with an Odyssey infrared imaging system (Li-Cor) using secondary antibodies, protocols and software (Odyssey 3.0) provided by

the manufacturer. Protein amounts per sample were determined using standard curves generated from the analysis of purified recombinant proteins analyzed in parallel. Average numbers of Env trimers per particle were calculated assuming an average of 2,400 CA or Gag molecules per particle (*26*).

Fab binding assay.

Gradient purified particles (2 μg of CA) were mixed with 1 μg 2G12 or Synagis Fab fragments in 25 μL final reaction volume. Samples were incubated for 1 hour at room temperature. Unbound Fab fragments were removed by ultracentrifugation through a 20% (w/w) sucrose cushion at 100,000 g for 2 h at 4 °C. Samples were separated by SDS-PAGE (12.5% acrylamide) and transferred onto a nitrocellulose membrane (Whatman) by semi-dry blotting. Membranes were blocked and probed for Env using a rabbit polyclonal anti-gp120 antiserum. Bound antibody was detected using anti-human IRDye800 conjugated Ab (Rockland Immunochem.) and quantitated using an Odyssey infrared imaging system (Li-Cor) using protocols and software (Odyssey 3.0) provided by the manufacturer.

Virus infectivity and entry assays

For single round infectivity assays, equal amounts (10 ng CA) of three independent virus preparations for both HIV-1 Env(wt) and HIV-1 Env(ΔCT) were used to infect SupT1R5 cells in duplicate (96-well plate, 2×10^5 cells/well). At 3 days post infection cells were harvested, washed with PBS and fixed with 3% PFA/PBS for 90 min. Cells were immunostained for intracellular HIV-1 CA protein using monoclonal antibody KC57-FITC (Beckman Coulter) in 0.1% TX100/ PBS and the proportion of CA expressing cells was determined by flow cytometry.

For endpoint titration, three independent experiments using independent virus preparations were performed. For each experiment, serial 10-fold dilutions of viruses carrying Env(wt) or Env(ΔCT), respectively, were used to infect C8166 cells in quadruplicate (96-well plate, 3×10^4 cells/well). At 8 days post infection wells containing a spreading virus infection were identified by the presence of syncytia and 50% tissue culture infectious dose (TCID50) was calculated

according to Spearman-Kärber.

Virus entry into PBMCs was measured by a modified β-lactamase (BlaM) fusion assay (*23*). PBMCs were prepared from buffy coats of healthy blood donors by Ficoll gradient centrifugation and stimulated with 2 μg/mL phytohemagglutinin and 10 ng/mL IL-2 for 4 days. PBMCs from three individual donors were incubated with equal amounts (50 ng CA) of mature or immature BlaM.Vpr reporter virus particles carrying Env(wt), Env(ΔCT), or no Env, respectively for 5 h. Virus was removed and cells were stained for β-lactamase activity using the fluorogenic BlaM substrate CCF-2 (Invitrogen) overnight at room temperature according to the manufacturer's instructions. Cleavage of CCF-2 by BlaM, delivered via entry of the reporter virus into the cytoplasm, leads to a shift of the dye's fluorescence emission maximum from 518 nm to 447 nm. The proportion of entry positive cells was determined by flow cytometry.

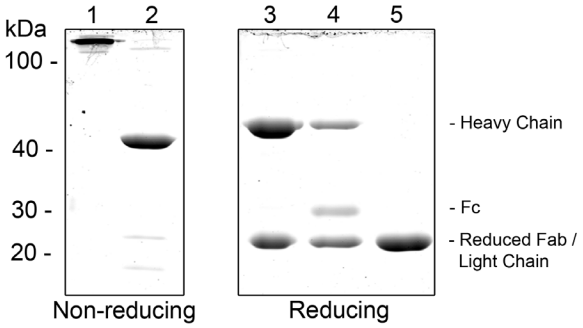

Fig. S1. SDS-PAGE analysis of purified 2G12 Fab fragments. Input IgG and papain digestion products were resolved by SDS-PAGE under non-reducing (lanes 1, 2) and reducing (lanes 3-5) conditions, respectively. Lanes: 1: 2G12 IgG, 2: Purified 2G12 Fab, 3: 2G12 IgG, 4: Papain digested 2G12 IgG before purification, 5: Purified 2G12 Fab.

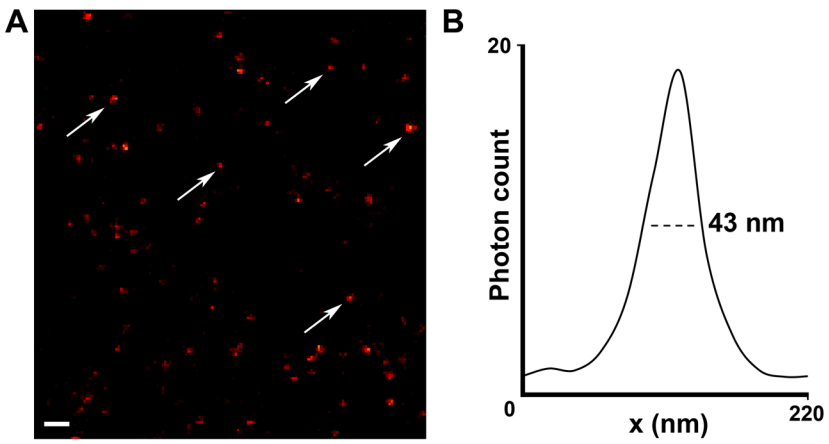

Fig. S2. Estimation of the effective resolution of the STED setup. (**A**) A raw image of recombinant monomeric Env protein labelled using 2G12 Fab and Atto 565 conjugated secondary Fab. Arrows indicate immunocomplexes used for the fluorescence intensity profile measurements. (**B**) An average fluorescence intensity profile for the recombinant monomeric Env immunocomplexes indicated in **A**. The effective resolution for this dye was estimated by FWHM measurement (dashed line). Scale bars: 200 nm.

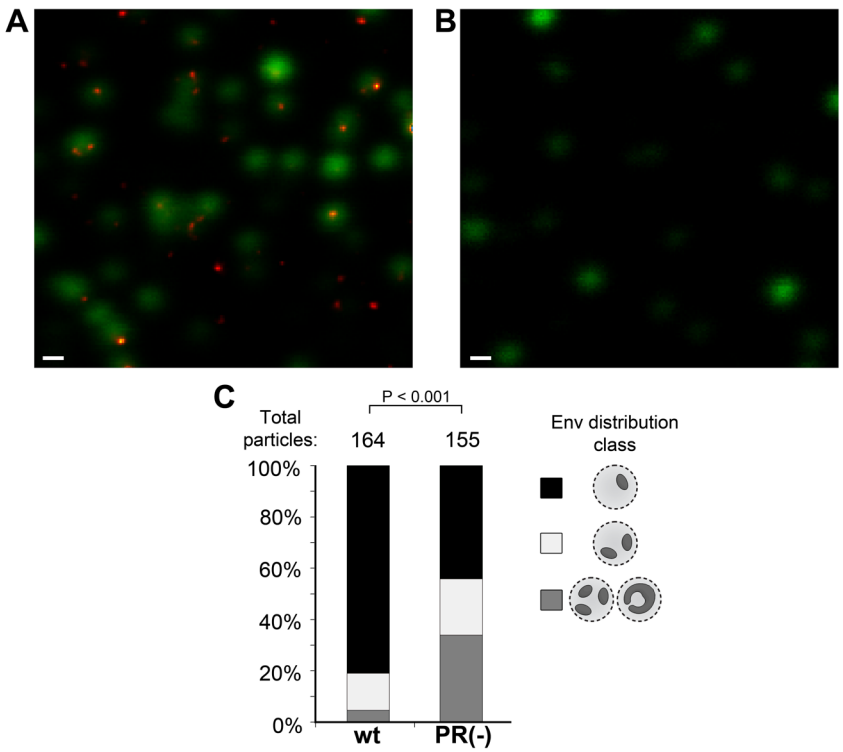

Fig. S3. STED visualization of HIV-1 Env distribution on purified particles using Fab b12. Particles containing eGFP.Vpr (green) were adhered to fibronectin coated cover slips and stained for Env using Fab b12 and Atto 565-labelled secondary Fab (orange). Images were acquired using the STED microscope setup, with the eGFP.Vpr signal recorded in the standard confocal mode to define the localization of particles. (**A, B**) Representative images of mature Env(wt) and negative control Env(-) virus preparations, respectively. Scale bars: 200 nm. (**C**) Env distribution patterns on mature (wt) and immature (PR-) particles stained with b12 Fab.

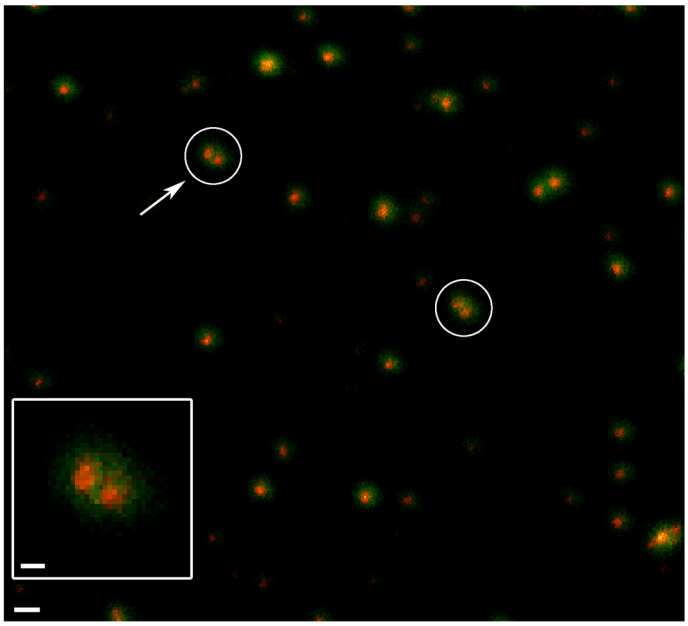

Fig. S4. Characterisation of the degree of aggregation of cover slip adhered HIV-1 particles by STED microscopy. Purified HIV-1 particles, containing eGFP.Vpr, were adhered to fibronectin coated cover slips. The eGFP signal was recorded using the GFP-STED microscope setup in the conventional diffraction limited (green) or STED (orange) mode, respectively. A representative image of a mature Env(wt) virus preparation is shown. Circles indicate examples of closely adjacent virus particles which were not resolved in the diffraction limited mode. Scale bar: 300 nm. Inset: A close-up view of the closely adjacent particles indicated by the arrow. Scale bar: 100 nm.

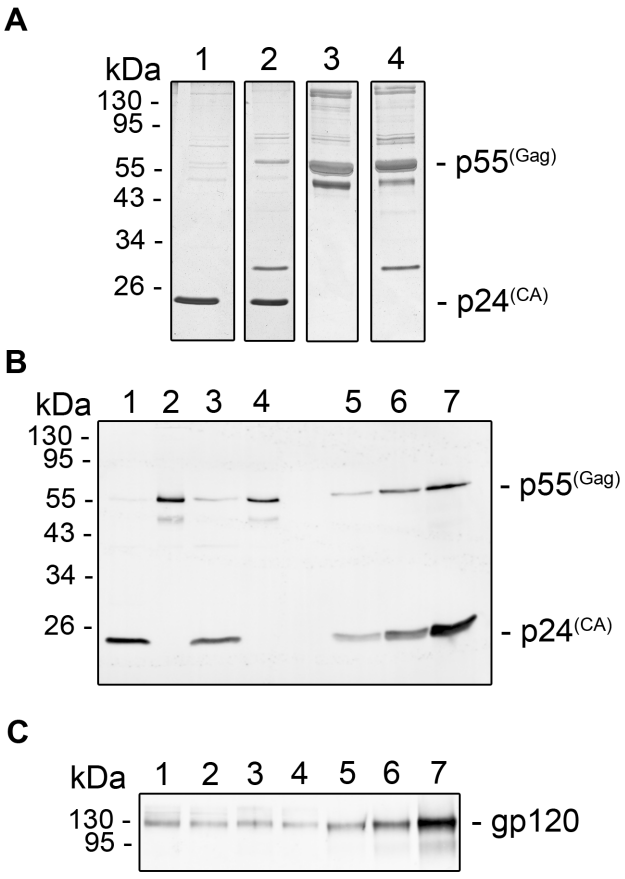

Fig. S5. Estimation of Env trimer incorporation by quantitative immunoblotting. **(A)** A silver stained SDS-PAGE showing the purity of gradient purified particles. Lanes: 1: mature HIV_{NL4-3}, 2: mature replication incompetent HIV, 3: immature HIV_{NL4-3}, 4: immature replication incompetent HIV. **(B)** A representative immunoblot used for the determination of the CA or Gag concentration of gradient purified virus samples. Proteins were detected using polyclonal sheep antiserum raised against recombinant HIV-1 CA. Lanes: 1: mature HIV_{NL4-3}, 2: immature HIV_{NL4-3}, 3: mature replication incompetent HIV, 4: immature replication incompetent HIV, 5-7: mixture of purified Gag and CA standards 10, 30 and 100 ng, respectively. **(C)** A representative immunoblot used for the determination of gp120 concentration of purified virus preparations. Proteins were detected using polyclonal rabbit antiserum against recombinant HIV-1 gp120. Lanes 1: mature HIV_{NL4-3}, 2: immature HIV_{NL4-3}, 3: mature replication incompetent HIV, 4: immature replication incompetent HIV, 5-7: recombinant Env (gp140) standard 0.1, 0.3 and 1 pmol, respectively.

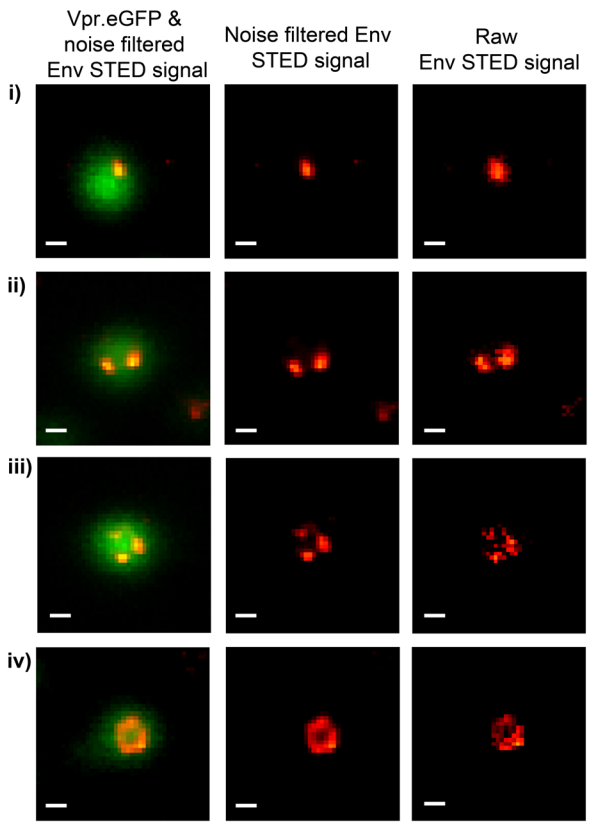

Fig. S6. Comparison of the raw and noise-filtered Env STED signal. Representative images of eGFP.Vpr (green) containing HIV-1 particles stained for Env (orange), displaying different Env distribution classes: (**i**) single Env focus, (**ii**) two Env foci, (**iii**, **iv**) three or more Env foci. The same particles as in Fig. 3 are shown with the right panels displaying the raw STED signal prior to noise filtering. Scale bars: 100 nm.

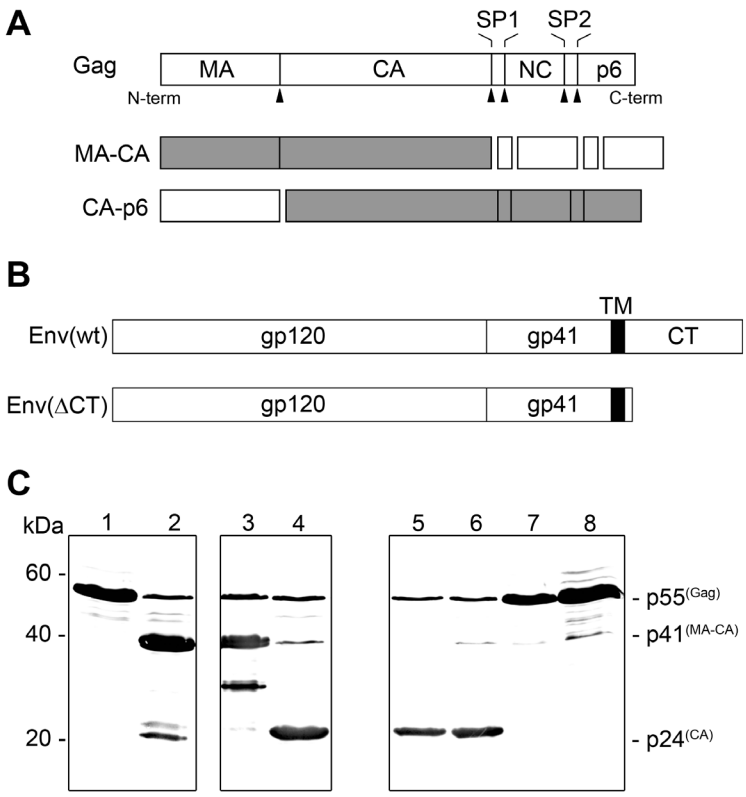

Fig. S7. Characterization of HIV-1 particles with defective Gag processing and particles pseudotyped with Env(wt) or Env(ΔCT), respectively. **(A)** Top: A schematic representation of the HIV-1 Gag polyprotein. Arrowheads indicate PR cleavage sites. Bottom: Gag derived products from the PR cleavage site mutants used in this study. Gray boxes indicate partially processed products. **(B)** Top: A schematic representation of the HIV-1 Env protein with indicated domains: gp120, gp41, transmembrane domain (TM) and C-terminal tail (CT). Bottom: C-terminal tail truncated mutant used in this study. **(C)** Immunoblot analysis of particles with partially defective Gag processing and of particles carrying Env(ΔCT). Gag-derived proteins were detected using sheep polyclonal antiserum against HIV-1 CA. Lanes 1-4: particles displaying different degrees of Gag processing 1: PR(-), 2: MA-CA, 3: CA-p6, 4: wt HIV. Lanes 5-8: mature and immature particles pseudotyped with Env(wt) or Env(ΔCT). 5: mature, Env(wt), 6: mature, Env(ΔCT), 7: PR(-) Env(wt), 8: PR(-) Env(ΔCT).

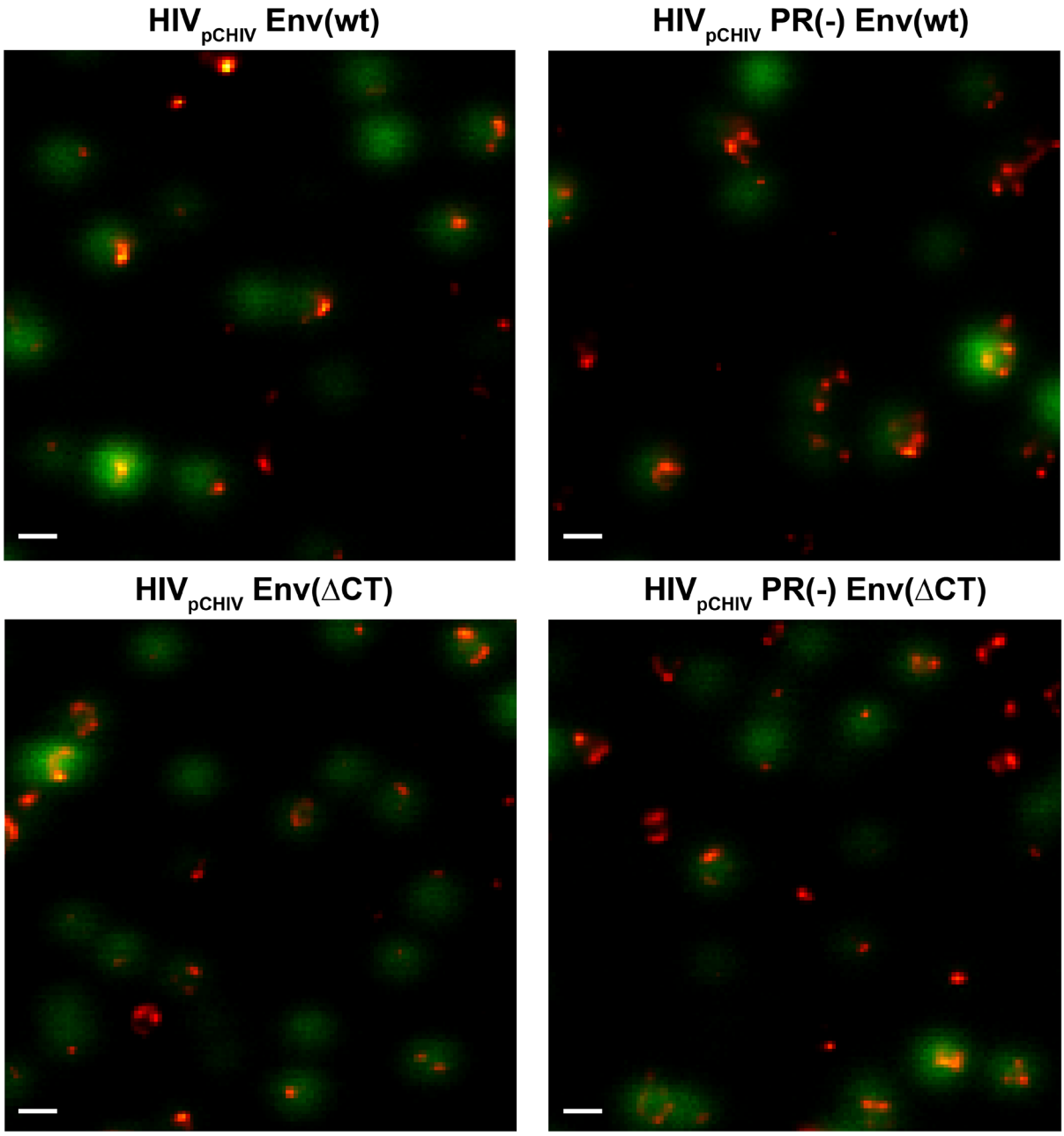

Fig. S8. Representative STED images of mature and immature HIV-1 particles pseudotyped with Env(wt) or Env(ΔCT). Purified HIV-1 particles, containing eGFP.Vpr (green), were adhered to fibronectin coated cover slips and stained for Env (orange). Images were acquired using the STED microscope, with the eGFP.Vpr signal recorded in the standard confocal mode to define the localization of particles and Env recorded in STED mode. Scale bars represent 200 nm.

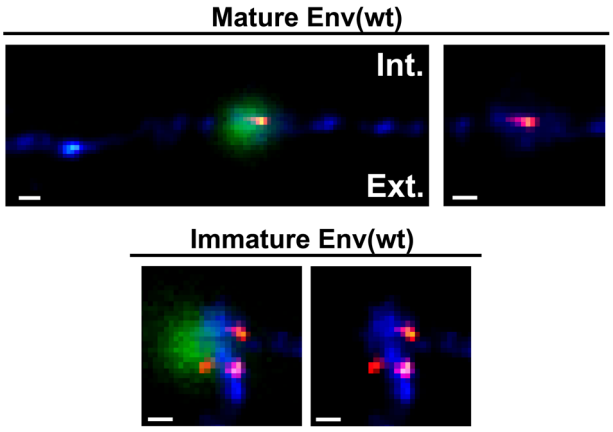

Fig. S9. Env distribution images of cell-attached HIV-1. Particles containing eGFP.Vpr (green) were pre-incubated with 2G12 Fab and allowed to attach to SupT1R5 cells followed by immunostaining for Env (orange) and cell surface CD4 (blue). Individual cell-attached particles were localized using the eGFP.Vpr signal in the confocal mode and Env/CD4 signals were analysed by a dual-color STED microscopy. Panels display cell-attached particles with eGFP/ Env/CD4 signal overlay (left) or Env/CD4 signal overlay (right). Scale bars: 100 nm.

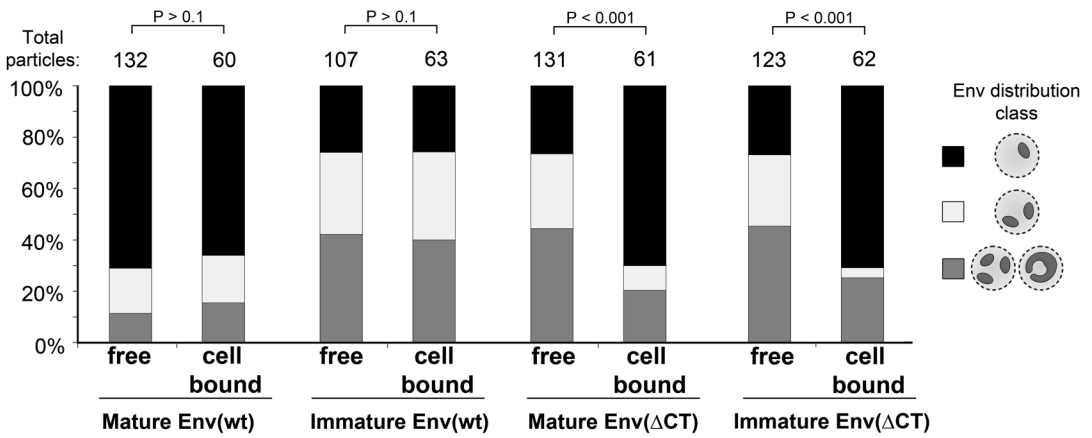

Fig. S10. Comparison of Env distribution on cell-free and cell-bound particles, respectively. The figure shows a comparison of mature and immature particles, pseudotyped with either Env(wt) or Env(ΔCT). It summarizes the data shown in main Figures 3 and 4 to allow better visualization of differences. The significance of differences was assessed by a Chi-squared test for independence at 2 degrees of freedom.

Particles	Env distribution class		
	Single focus	Two foci	Three or more foci
wt	69±4.4%	18±1.7%	12±5.5%
PR(-)	28±1.9%	24±1.6%	48±0.3%
MA-CA	36±6.4%	35±5.3%	30±1.3%
CA-p6	53±6.3%	27±5.4%	20±11.8%
Env(wt)	71±10.3%	17±4.6%	11±9.8%
PR(-) Env(wt)	26±2.7%	32±9.5%	42±12.1%
Env(ΔCT)	27±6.5%	29±7.7%	44±2.2%
PR(-) Env(ΔCT)	27±4.8%	28±2.9%	46±5.5%

Table S1. Mean and standard deviation of percentage values of Env distribution classes shown in Fig. 3. To minimize bias associated with manual assignment of Env distribution class, three independent blinded evaluations were performed. The table shows mean and SD values from these three evaluations for all data sets.

References and Notes

1. P. Cosson, Direct interaction between the envelope and matrix proteins of HIV-1. *EMBO J.* **15**, 5783 (1996). Medline
2. E. O. Freed, M. A. Martin, Domains of the human immunodeficiency virus type 1 matrix and gp41 cytoplasmic tail required for envelope incorporation into virions. *J. Virol.* **70**, 341 (1996). Medline
3. T. Murakami, E. O. Freed, The long cytoplasmic tail of gp41 is required in a cell type-dependent manner for HIV-1 envelope glycoprotein incorporation into virions. *Proc. Natl. Acad. Sci. U. S. A.* **97**, 343 (2000). doi:10.1073/pnas.97.1.343 Medline
4. E. Chertova *et al.*, Envelope glycoprotein incorporation, not shedding of surface envelope glycoprotein (gp120/SU), Is the primary determinant of SU content of purified human immunodeficiency virus type 1 and simian immunodeficiency virus. *J. Virol.* **76**, 5315 (2002). doi:10.1128/JVI.76.11.5315-5325.2002 Medline
5. P. Zhu *et al.*, Electron tomography analysis of envelope glycoprotein trimers on HIV and simian immunodeficiency virus virions. *Proc. Natl. Acad. Sci. U. S. A.* **100**, 15812 (2003). doi:10.1073/pnas.2634931100 Medline
6. R. H. Cheng *et al.*, Nucleocapsid and glycoprotein organization in an enveloped virus. *Cell* **80**, 621 (1995). doi:10.1016/0092-8674(95)90516-2 Medline
7. A. Harris *et al.*, Influenza virus pleiomorphy characterized by cryoelectron tomography. *Proc. Natl. Acad. Sci. U. S. A.* **103**, 19123 (2006). doi:10.1073/pnas.0607614103 Medline
8. P. Zhu *et al.*, Distribution and three-dimensional structure of AIDS virus envelope spikes. *Nature* **441**, 847 (2006). doi:10.1038/nature04817 Medline
9. A. Helenius, Unpacking the incoming influenza virus. *Cell* **69**, 577 (1992). doi:10.1016/0092-8674(92)90219-3 Medline
10. T. Murakami, S. Ablan, E. O. Freed, Y. Tanaka, Regulation of human immunodeficiency virus type 1 Env-mediated membrane fusion by viral protease activity. *J. Virol.* **78**, 1026 (2004). doi:10.1128/JVI.78.2.1026-1031.2004 Medline
11. D. J. Wyma *et al.*, Coupling of human immunodeficiency virus type 1 fusion to virion maturation: A novel role of the gp41 cytoplasmic tail. *J. Virol.* **78**, 3429 (2004). doi:10.1128/JVI.78.7.3429-3435.2004 Medline
12. N. Kol *et al.*, A stiffness switch in human immunodeficiency virus. *Biophys. J.* **92**, 1777 (2007). doi:10.1529/biophysj.106.093914 Medline
13. S. W. Hell, J. Wichmann, Breaking the diffraction resolution limit by stimulated emission: Stimulated-emission-depletion fluorescence microscopy. *Opt. Lett.* **19**, 780 (1994). doi:10.1364/OL.19.000780 Medline

14. A. Trkola *et al.*, Human monoclonal antibody 2G12 defines a distinctive neutralization epitope on the gp120 glycoprotein of human immunodeficiency virus type 1. *J. Virol.* **70**, 1100 (1996). Medline
15. P. Roben *et al.*, Recognition properties of a panel of human recombinant Fab fragments to the CD4 binding site of gp120 that show differing abilities to neutralize human immunodeficiency virus type 1. *J. Virol.* **68**, 4821 (1994). Medline
16. D. McDonald *et al.*, Visualization of the intracellular behavior of HIV in living cells. *J. Cell Biol.* **159**, 441 (2002). doi:10.1083/jcb.200203150 Medline
17. J. A. Briggs, T. Wilk, R. Welker, H. G. Krausslich, S. D. Fuller, Structural organization of authentic, mature HIV-1 virions and cores. *EMBO J.* **22**, 1707 (2003). doi:10.1093/emboj/cdg143 Medline
18. T. Endress *et al.*, HIV-1-cellular interactions analyzed by single virus tracing. *Eur. Biophys. J.* **37**, 1291 (2008). doi:10.1007/s00249-008-0322-z Medline
19. A. de Marco *et al.*, Structural analysis of HIV-1 maturation using cryo-electron tomography. *PLoS Pathog.* **6**, e1001215 (2010). doi:10.1371/journal.ppat.1001215 Medline
20. M. J. Forster, B. Mulloy, M. V. Nermut, Molecular modelling study of HIV p17gag (MA) protein shell utilising data from electron microscopy and X-ray crystallography. *J. Mol. Biol.* **298**, 841 (2000). doi:10.1006/jmbi.2000.3715 Medline
21. S. F. Lee *et al.*, Multimerization potential of the cytoplasmic domain of the human immunodeficiency virus type 1 transmembrane glycoprotein gp41. *J. Biol. Chem.* **275**, 15809 (2000). doi:10.1074/jbc.M000601200 Medline
22. T. Wilk, T. Pfeiffer, V. Bosch, Retained in vitro infectivity and cytopathogenicity of HIV-1 despite truncation of the C-terminal tail of the env gene product. *Virology* **189**, 167 (1992). doi:10.1016/0042-6822(92)90692-I Medline
23. M. Cavrois, C. De Noronha, W. C. Greene, A sensitive and specific enzyme-based assay detecting HIV-1 virion fusion in primary T lymphocytes. *Nat. Biotechnol.* **20**, 1151 (2002). doi:10.1038/nbt745 Medline
24. R. Sougrat *et al.*, Electron tomography of the contact between T cells and SIV/HIV-1: Implications for viral entry. *PLoS Pathog.* **3**, e63 (2007). doi:10.1371/journal.ppat.0030063 Medline
25. D. Holtkotte, T. Pfeiffer, T. Pisch, V. Bosch, Selection and characterization of a replication-competent human immunodeficiency virus type 1 variant encoding C-terminally truncated env. *AIDS Res. Hum. Retrov.* **22**, 57 (2006). doi:10.1089/aid.2006.22.57 Medline
26. L. A. Carlson *et al.*, Three-dimensional analysis of budding sites and released virus suggests a revised model for HIV-1 morphogenesis. *Cell Host Microbe* **4**, 592 (2008). doi:10.1016/j.chom.2008.10.013 Medline

27. M. Lampe *et al.*, Double-labelled HIV-1 particles for study of virus-cell interaction. *Virology* **360**, 92 (2007). doi:10.1016/j.virol.2006.10.005 Medline
28. B. Muller *et al.*, HIV-1 Gag Processing Intermediates Trans-dominantly Interfere with HIV-1 Infectivity. *J. Biol. Chem.* **284**, 29692 (2009). doi:10.1074/jbc.M109.027144 Medline
29. A. Adachi *et al.*, Production of acquired immunodeficiency syndrome-associated retrovirus in human and nonhuman cells transfected with an infectious molecular clone. *J. Virol.* **59**, 284 (1986). Medline
30. S. Harada, Y. Koyanagi, N. Yamamoto, Infection of HTLV-III/LAV in HTLV-I-carrying cells MT-2 and MT-4 and application in a plaque assay. *Science* **229**, 563 (1985). doi:10.1126/science.2992081 Medline
31. R. E. Means *et al.*, Ability of the V3 loop of simian immunodeficiency virus to serve as a target for antibody-mediated neutralization: correlation of neutralization sensitivity, growth in macrophages, and decreased dependence on CD4. *J. Virol.* **75**, 3903 (2001). doi:10.1128/JVI.75.8.3903-3915.2001 Medline
32. M. Dettenhofer, X. F. Yu, Highly purified human immunodeficiency virus type 1 reveals a virtual absence of Vif in virions. *J. Virol.* **73**, 1460 (1999). Medline
33. T. J. Holmes, Y.-H. Liu, Richardson lucy/maximum likelihood image restoration algorithm for fluorescence microscopy: further testing. *Appl. Optics* **28**, 4930 (1989). doi:10.1364/AO.28.004930 Medline